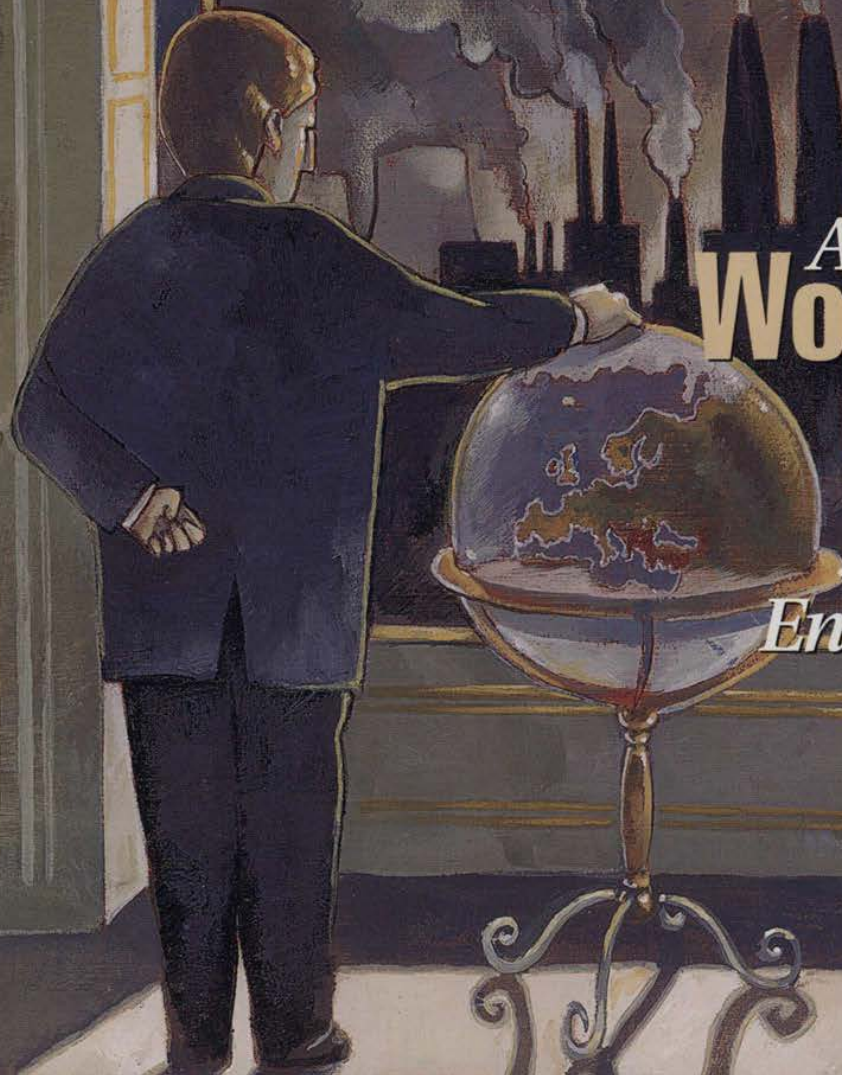


February 1, 2000

# ENVIRONMENTAL Science & Technology

<http://pubs.acs.org/est>



**A**  
**Worrisome**  
**Outlook**  
*for Europe's*  
*Environment?*

PUBLISHED BY  
THE AMERICAN  
CHEMICAL SOCIETY

**European ban on use of surfactant alarms U.S. producers • 68A**

U.S. chemical producers sharply criticized a draft EU risk assessment that recommends a European ban on many uses of nonylphenol ethoxylates.

**Growing conflict over GM trees • 69A**

As the number of genetically modified trees being planted in test plots has increased, debate over their pros and cons has grown more heated, concurrent with a rise in vandalism against research laboratories.

**European governments urged to consider environmental benchmarks • 70A**

The European Environment Bureau hopes that government leaders will base environmental performance on specified targets, timetables, and indicators in 10 key areas.

**EPA's diesel health assessment needs tweaking, science advisors say • 71A**

EPA's Clean Air Act Scientific Advisory Committee has again declined approval of the Agency's analysis of human health effects from diesel exhaust.

**News Briefs • 72A**

Market-based pollution control alternatives • Waste reduction • Risks of contaminated underwater sediments • Paper in catalogs • Conservation areas threatened • Chemical accidents • Pollutant-birth defect link • School bus pollution

**Departments****Comment • 63A**

How to thank our reviewers

**EPA Watch • 73A**

2000 budget includes steady funding; policy orders • PBT releases, including dioxin, will be captured on TRI reports • Confusion over agreement confounds species protection efforts • Proposal to regulate large animal farms still under fire

**Technology Update • 75A**

Technology costs for arsenic removal

**Research Watch • 91A**

Huge dioxin emission source • Controlling mercury emissions

**Online/In Print • 93A**

Web sites and new books

**Meeting Calendar • 94A**

New events through April 2000

**Classifieds • 95A**

Environmental career opportunities • Advertiser index

**Research at a Glance**

Aminodinitrotoluene, kinetics, 450  
Aminodinitrotoluene, oxidation, 497  
Atrazine, degradation, 430  
Bacterial bioremediation, 535  
Biofilters, performance, 461  
Chlorobenzene, in sediments, 385  
Chloronaphthalenes, in air, 393  
Chromium, leaching, 455  
Cr(VI), reduction, 438  
Diesel fuels, emissions, 349  
Haloorganics, FeS, 422  
Hydrocarbons, degradation, 489  
Iodide, sorption, 399  
Mercury, sequestration, 483  
MTBE, outboard engines, 368  
n-Alkanes, solubilization, 476  
Nitroaromatics, reactions, 505  
NOM, aromatics, 444  
PAHs, in air, 356  
PCBs, contamination, 527  
PCDD/DFs, source, 377  
Pesticides, in air, 393  
Phenanthrene, sorption, 406  
Phenol, degradation, 509  
Pyrene, photochemistry, 415  
SOM, composition, 530  
Sorption, mechanisms, 468  
SVOCs, precipitation, 361  
TCE, dechlorination, 514  
Trees, pollution damage, 373  
Wastewater, treatment, 522

The table of contents of research papers in this issue begins on page 61A.



**Cover:** Maria Burke reviews a new European Environment Agency report, which finds that environmental policies have not achieved desired objectives. (Artwork by Matthew J. Baek)

34(3) 57A-96A/349-540  
ISSN 0013 936X

# Optimization of High Temperature Sulfur Impregnation on Activated Carbon for Permanent Sequestration of Elemental Mercury Vapors

WEI LIU AND RADISAV D. VIDIC\*

Department of Civil and Environmental Engineering,  
943 Benedum Hall, University of Pittsburgh,  
Pittsburgh, Pennsylvania 15261-2294

THOMAS D. BROWN

U.S. Department of Energy, Federal Energy Technology Center,  
P.O. Box 10940, Pittsburgh, Pennsylvania 15236-0940

Following previous success with the use of activated carbon impregnated with sulfur at elevated temperatures for elemental mercury control, possible improvements in the impregnation procedure were evaluated in this study. Adsorbents prepared by thoroughly mixing sulfur and activated carbon in the furnace at the initial sulfur-to-carbon ratio (SCR) ranging from 4:1 to 1:2 showed similar adsorptive behavior in a fixed-bed system. Maintaining a stagnant inert atmosphere during the impregnation process improves sulfur deposition resulting in the enhanced dynamic capacity of the adsorbent when compared to other sulfur impregnated carbons. The fate of spent adsorbents was assessed using a toxicity characteristics leaching procedure (TCLP). Although mercury concentration in all leachates was below the TCLP limit (0.2 mg/L), virgin activated carbon lost a significant fraction of the adsorbed elemental mercury during storage, while no loss was observed for sulfur-impregnated carbons. This finding suggests that virgin activated carbon may not be appropriate adsorbent for permanent sequestration of anthropogenic elemental mercury emissions.

## Introduction

As listed in the Clean Air Act Amendments of 1990, mercury is one of the 189 hazardous air pollutants (HAPs). Although air emissions of mercury occur naturally, major mercury pollution comes from anthropogenic activities. Recent EPA report showed that coal-fired power plants, municipal waste combustors, and medical waste incinerators account for more than 70% of the total anthropogenic mercury emissions (1).

Mercury emission control measures in coal-fired power plants are mainly based on the existing air pollution control devices (APCD). The primary APCDs include multiple cyclones, electrostatic precipitators (ESPs), fabric filters (baghouses), wet scrubbers, and wet and dry flue gas desulfurization (FGD) systems. Several studies revealed that the efficiency of mercury control is a function of a specific device used and flue gas conditions. For example, the oxidized mercury could be trapped to a substantial degree by fabric

filters, while elemental mercury could not be captured due to its small diameter. The average removal efficiency of total mercury for fabric filter was about 30% (2). A series of pilot plants studies on wet scrubbing FGD system has shown that 90% HgCl<sub>2</sub> was removed from flue gas, while essentially no elemental mercury was dissolved in the scrubbing slurry (3).

New technologies are being developed for the control of mercury emissions. Among them, activated carbon adsorption demonstrated potential for capturing both elemental and oxidized mercury species.

Vidic and McLaughlin (4) found that sulfur impregnated carbon performed much better than virgin carbon. Physisorption dominated the capacity of a virgin carbon, while HgS formation controlled the adsorption ability of sulfur-impregnated carbons. Additional study (5) showed that the improved mercury uptake capacity by sulfur-impregnated carbon was also related to the factors such as bonding between sulfur and carbon surface, specific surface area of the carbon, and types of sulfur allotropes impregnated on the carbon surface. Liu et al. (6) further developed this new impregnation protocol to control the parameters (temperature and initial sulfur-to-carbon ratio) that have the major impact on the performance of sulfur-impregnated activated carbons. It was found that the impregnation temperature was the crucial parameter for the performance of sulfur-impregnated carbons, while the amount of sulfur impregnated on the carbon surface had much lower impact. This was explained by the presence of more short chain sulfur allotropes, larger surface area, and larger fraction of meso-pores in the adsorbents prepared at higher temperatures.

One of the major drawbacks of the impregnation procedure used in previous studies (5, 6) was that only 3% of the sulfur used in the procedure was impregnated onto activated carbon. Therefore, one objective of this study was to develop an improved impregnation method that would reduce the sulfur loss while producing equally effective mercury adsorbents. This is done by determining the impact of impregnation process modifications and adsorbent particle size on sulfur deposition and adsorbent performance for elemental mercury uptake.

Current approaches to handling the spent adsorbents include ash pond or landfill disposal or regeneration. Powdered activated carbon injection technology does not allow for the recovery and regeneration of spent adsorbent which is, instead, discharged together with fly ash directly into a pond. For granular activated carbon, both landfilling and regeneration are feasible. Upon disposal of saturated adsorbents, the adsorbed mercury compounds may be dissolved into leachate due to acidic conditions that occur during landfill stabilization. Once mercury compounds are mobilized, their migration could pose significant environmental risk. The second objective of this study was to investigate the environmental impact of mercury-saturated adsorbents after they are removed from the system. Toxicity characteristics leaching procedure (TCLP) (40 CFR 261) was utilized in order to evaluate the fate of the adsorbed mercury compounds once saturated adsorbents are removed from the flue gas.

## Experimental Methods

BPL, a commercially available bituminous coal-based activated carbon, was provided by the manufacturer (Calgon Carbon Corporation, Pittsburgh, PA) in 4 × 10 and 12 × 30 U.S. mesh sizes and was used as base adsorbent throughout

\* Corresponding author phone: (412)624-1307; fax: (412)624-0135; e-mail: vidic@engr.pitt.edu.

the study. It was ground into 60 × 80, 170 × 230, and minus 400 U.S. mesh size and stored in a desiccator prior to use.

Two sulfur impregnation procedures similar to the method described previously (5, 6) were used in this study. The major difference is that instead of using two ceramic boats, one for sulfur and one for activated carbon, only one boat was used. Sulfur flakes were ground into a fine powder and thoroughly mixed with carbon in a single boat. The initial sulfur-to-carbon ratio (SCR) in the boat was adjusted from 4:1 to 1:5, and the impregnation temperature was set at 600 °C for all tests. The designation of these carbons used a letter M to indicate that the sulfur and carbon were mixed in one ceramic boat. For example, BPL-S-4/1M-600 denotes a BPL carbon impregnated with sulfur at 600 °C with an SCR of 4:1.

The second procedure also used single boat for the impregnation procedure, and the SCR was set at 1:2. However, after an inert atmosphere was created inside the system, nitrogen flow was stopped, the tube furnace was sealed, and a balloon was attached to the furnace exit to compensate for gas expansion. The furnace temperature was raised to 600 °C and held at that level for 2 h. The objective of this method was to further increase the amount of active sulfur molecules on the carbon surface. The designation of this adsorbent was BPL-S-1/2M-600S.

When 170 × 230 and minus 400 U.S. mesh size carbons were used for the preparation of sulfur-impregnated carbons adsorbents, the impregnation conditions were identical to those described previously for BPL-S adsorbents (5, 6) to allow for direct assessment of the impact of carbon particle size on sulfur impregnation process and resulting mercury uptake dynamics.

The sulfur content of all adsorbents was measured using a Leco Model SC 132 sulfur determinator (Leco Corporation, St. Joseph, MI), while surface areas were determined using an Orr Surface-Area Pore-Volume Analyzer Model 2100 (Micromeritics Instrument Corporation, Atlanta, GA) and calculated using the nitrogen BET isotherm method.

Adsorbent samples were subjected to FTIR analysis in an attempt to elucidate predominant sulfur forms resulting from these impregnation procedures. Samples for IR analysis were prepared by grinding a very small amount of adsorbent with KBr salt followed by compression between two stainless steel cylinders to form a thin transparent solid film. This film was subjected to direct scanning in an FTIR spectrophotometer (Mattson IR, Madison Instruments, Inc. Madison, WI) to determine predominant forms of sulfur on the carbon surface.

Mercury uptake by these newly developed sulfur impregnated adsorbents was studied using a fixed-bed adsorber system in order to assess the impact of modifications in sulfur impregnation procedure on their performance. All column tests were conducted using a 1/4 in. (0.635 cm) I.D. stainless steel reactor charged with 100 mg of impregnated carbon and operated at 140 °C in a downflow mode. Pure N<sub>2</sub> at a flow rate of 1.0 L/min was used as the carrier gas in all experiments so that the results can be compared to previous data (5, 6). Unless otherwise noted, influent mercury concentration was 55 µg/m<sup>3</sup>.

EPA Method 1311 was used to select the proper extraction fluid for TCLP analysis. Based on the tests with various adsorbents, it was found that the extraction fluid 1 (5.7 mL of glacial CH<sub>3</sub>CH<sub>2</sub>OOH and 64.3 mL of 1 N NaOH in 1.0 L of reagent water, pH = 4.93 ± 0.05, EPA Method 1311) was suitable for the extraction of mercury loaded adsorbents.

## Results and Discussion

**FTIR Analyses of Virgin and Sulfur Impregnated Carbons.** It has long been assumed that the sulfur impregnated on the carbon surface was in the elemental form. However, early research has shown that the actual forms of sulfur on the adsorbent surface could change from simple elemental sulfur

to various sulfur compounds (7). The actual carbon-sulfur complexes were strongly related to the initial structures of carbon. For example, hydrogen sulfide and organic sulfur compounds were found if the carbons contained hydrocarbon compounds (8).

FTIR was used to measure possible sulfur functional groups of on the carbon surface. Figures 1 and 2 depict IR scans of virgin BPL and BPL-S-4/1-600, respectively. As expected, Figure 1 revealed no distinct sulfur-related peaks on virgin BPL because its total sulfur content was below 1%. FTIR analysis of BPL-S-4/1-600 also revealed no distinct sulfur-related peaks (Figure 2) throughout 500–4000 cm<sup>-1</sup>, where the possible ranges for sulfur-based functional groups are as follows (9):

functional group	possible peaks, cm <sup>-1</sup>
S-H	1200–1400, 3700–4000
S-C	1300–1400, 1500–1600
S-O	1100–1300, 1600–1700

The predominant sulfur bonds that are expected in these novel adsorbents are S-C and possibly some S-H and S-O. In addition to the fact that all of these bonds have fairly weak vibrations (9), extremely high background noise in the fingerprint region and overwhelming O-H and C-H vibrations coming from the surface of activated carbon, as evidenced from the spectra of virgin BPL carbon in Figure 1, precluded the observation of such bonds. However, under high impregnation temperature (600 °C), most sulfur-based compounds that could be formed on the carbon surface would evaporate or decompose to simple compounds that would be carried out of the furnace by the purge gas. This is particularly true for the simple sulfur compounds such as H<sub>2</sub>S, CS<sub>2</sub>, or SO<sub>2</sub> that could easily be volatilized and flushed out of the system. It is reasonable to assume that the major sulfur forms on the carbon surface resulting from sulfur impregnation at elevated temperatures are short linear-chain sulfur allotropes as suggested by Korpel and Vidic (5).

**Performance of BPL-S-M Series.** As can be seen from Figure 3, mercury uptakes by BPL-S-1/1M-600 and BPL-S-1/2M-600 are very close to that previously measured for BPL-S-4/1-600 (2300 µg Hg/g carbon) (6). However, the adsorptive capacity for mercury decreased to 1450 µg Hg/g carbon when the initial sulfur-to-carbon ratio was reduced to 1:5.

Sulfur content and specific surface area of these novel adsorbents are shown in Table 1. This table shows that all BPL-S and BPL-S-M adsorbents had very similar surface areas regardless of the impregnation method or SCR used. Furthermore, the sulfur content of BPL-S-M carbons prepared using the SCR of 1:1 and 1:2 is very close to that of BPL-S-4/1-600 (approximately 10%). Hence, all three adsorbents exhibited very similar behavior for the uptake of elemental mercury. Although BPL-S-1/5M-600 had similar BET surface area with other adsorbents, its sulfur content was about 20% lower, which can explain somewhat reduced capacity for elemental mercury.

The key advantage of the new impregnation procedure is that it reduced the amount of sulfur required to maintain sulfur content of about 10%. In our previous study, sulfur and carbon were kept in separate ceramic boats, and the majority of sulfur would be carried out of the furnace by N<sub>2</sub> gas before it had a chance to react with carbon. Furthermore, several mass transfer steps were required before sulfur impregnation onto carbon surface. The initial sulfur loss and mass transfer resistance are reduced for the newly developed methods since sulfur and carbon were thoroughly mixed in a single boat.

**Performance of BPL-S-1/2M-600S.** Figure 4 shows that the mercury uptake by BPL-S-1/2M-600S was about 10% higher when compared to BPL-S-4/1-600. Table 1 shows that

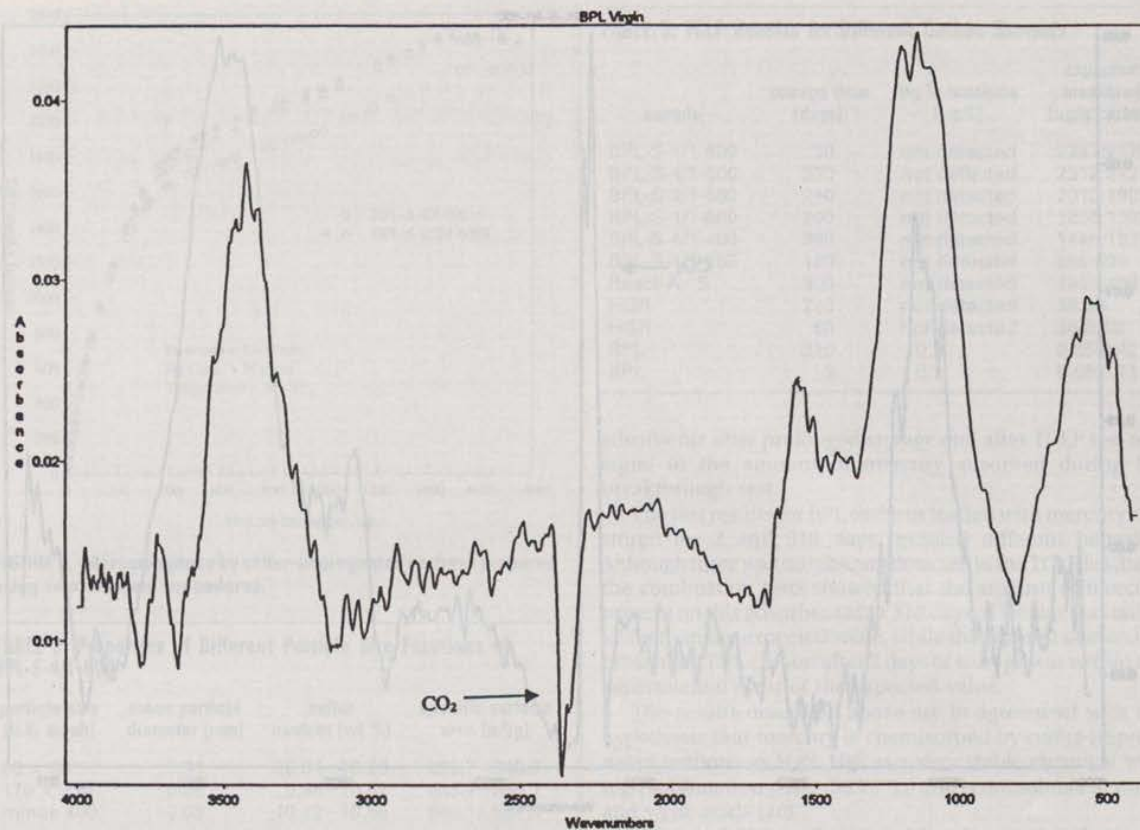


FIGURE 1. IR analysis of BPL surface for possible sulfur structures.

the sulfur content of BPL-S-1/2M-600S was about 20% higher than for the other carbons. Since all the carbons were prepared at same temperature, the predominant forms of sulfur allotropes should be the same (short chain sulfur molecules). Therefore, the amount of active sulfur molecules is proportional to the total sulfur content. Because of the higher sulfur content, BPL-S-21/2M-600S showed slightly better performance. On the other hand, Table 1 also shows that the surface area of this carbon was somewhat lower when compared to other carbons, which was most likely caused by the larger amount of sulfur deposited on the carbon surface. Reduction in surface area would normally offset the effect of having more active sulfur molecules. Furthermore, although the initial SCR used in the production of this carbon was 1:2, only about 20% of the sulfur was deposited on the carbon surface. Significant sulfur loss even in this procedure was probably due to the extreme high impregnation temperature.

The most likely explanation for the incomplete deposition of sulfur on the carbon surface even in a closed system used for the production of BPL-S-21/2M-600S is insufficient reaction time. During a 2-h period when the furnace temperature was maintained at 600 °C only about 20% of the sulfur was deposited on the surface of activated carbon, and, except for the amount that diffused through the balloon, the unreacted sulfur remained in the vapor phase inside the quartz tube. The unreacted sulfur vapor was deposited on the walls of the quartz tube during the cooling phase as evidenced by yellow discoloration. It is possible that longer impregnation time would result in better sulfur utilization and improved economics of the process.

**Effect of Adsorbent Particle Size.** Data shown in Table 2 indicate that there is no significant difference in sulfur content and specific surface area among the three particle

size fractions used in this study. However, Figure 5 shows that smaller particle size adsorbents exhibited higher dynamic adsorptive capacity when compared to 60 × 80 U.S. mesh size BPL-S-4/1-600. It is clear that Figure 5 does not reflect a true adsorption equilibrium because the adsorbent particle size should not have such a pronounced impact on the adsorption capacity, especially considering that all fractions had very similar surface area and sulfur content. The data shown in Figure 5 reflect a dynamic equilibrium that is established for a given set of fixed-bed operating parameters (e.g., temperature, influent composition, empty bed contact time, adsorbent particle size, etc.) and is defined by the lack of additional measurable mercury uptake. Korpiel and Vidic (5) argued that the dynamic equilibrium established in a single breakthrough test does not reflect the true capacity of sulfur impregnated adsorbents for mercury because the rate of mercuric sulfide formation and subsequent diffusion into the sulfur bulk phase is the rate limiting step in the adsorption dynamics. Rapid formation of large HgS molecules which can block the access to the narrower pores and prevent mercury molecules from accessing the highly reactive S<sub>2</sub> molecules that are present in the microporous region of the BPL-S carbon is responsible for the apparently low sulfur utilization in a single breakthrough test. They also showed that even after 100% breakthrough was observed in a given breakthrough test, additional mercury uptake would occur in subsequent loading steps when HgS formed in the previous loading step was allowed sufficient time to diffuse into the bulk sulfur.

It is obvious that the reduction in the adsorbent particle size from 60 × 80 (0.21 mm) to 170 × 230 (0.08 mm) U.S. mesh size provided sufficient kinetic advantage in a fixed-bed operated at an extremely short empty bed contact time of 0.011 seconds to allow better penetration of mercury

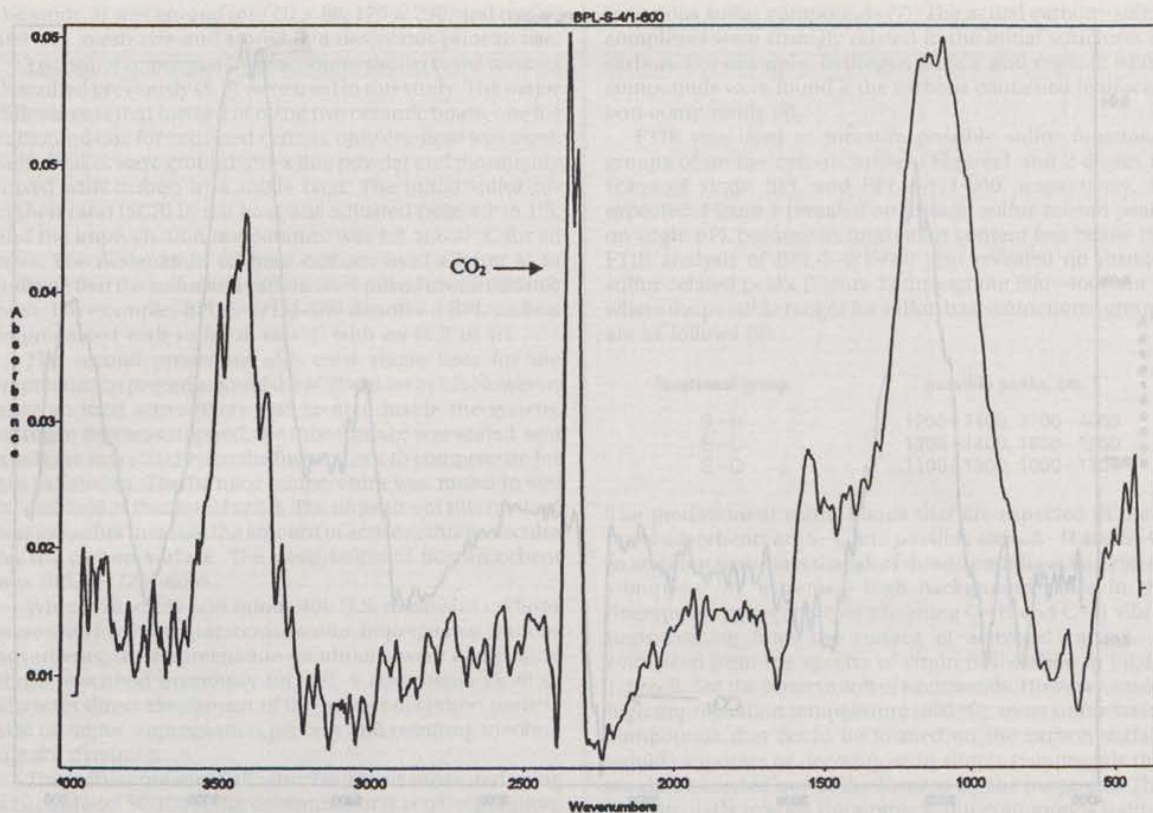


FIGURE 2. IR analysis of BPL-S-4/1-600 surface for possible sulfur structures.

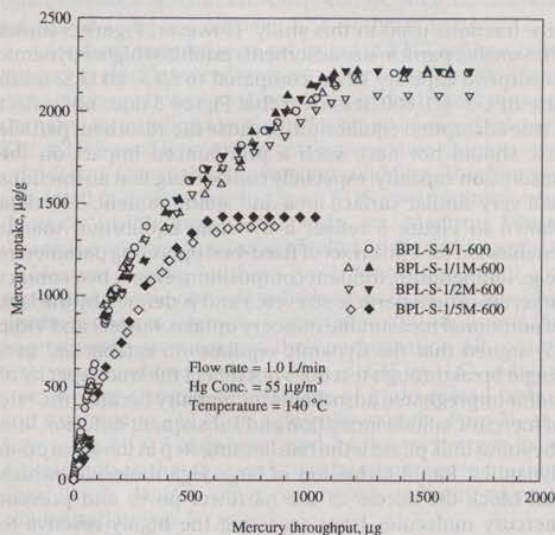


FIGURE 3. Mercury uptake by BPL-S-M adsorbents.

molecules into the microporous region before HgS formation prevented the remaining sulfur molecules to react with mercury. However, no additional increase in capacity was observed as the particle size decreased from  $170 \times 230$  (0.08 mm) to minus 400 (0.03 mm) U.S. mesh size. It is very likely that the kinetic limitations of a short empty bed contact time are fully counterbalanced by the reduction in particle size from  $60 \times 80$  to  $170 \times 230$  and that further particle size reduction brings no benefits to the process of mercury uptake. It is also possible that further reduction in empty bed contact

TABLE 1. Sulfur Content and Surface Area of Sulfur Impregnated Carbons

adsorbent	sulfur content [wt %]	specific surface area [m <sup>2</sup> /g]
BPL	0.5–0.7	988–1026
BPL-S-4/1-600	10.0–10.2	824–846
BPL-S-1/1M-600	10.9–11.0	842–871
BPL-S-1/2M-600	9.4–9.8	854–905
BPL-S-1/5M-600	7.9–8.0	857–862
BPL-S-1/2M-600S	12.5–12.9	789–812

time could bring about advantages of using even smaller adsorbent particle size.

**Fate of Spent Adsorbents.** To determine the fate of mercury adsorbed on activated carbon-based adsorbents, a TCLP test was conducted by placing 0.1 g of spent adsorbent in a glass vial together with 20 mL of extraction fluid 1. The volume of the vial was also 20 mL so that there would be no headspace above the liquid. By doing so, the possibility of losing any mercury into the vapor phase can be eliminated. All the sample vials were capped and sealed tightly by Teflon tapes. Then, the vials were placed in a 30 rpm tumbler for 18–20 h of the extraction process.

The supernatant was separated by pressurized filtration and liquid mercury analysis method (5) was used to measure mercury concentration in the leachate. The solid adsorbent was collected to verify the remaining mercury concentration by combusting the adsorbent in oxygen atmosphere at 800 °C. The combustion off-gas was collected in impingers (15 g of  $\text{KMnO}_4$  in 1 L of 10%  $\text{H}_2\text{SO}_4$ ) that were analyzed by liquid mercury analysis method.

Table 3 shows the mercury concentrations measured in extracts of different spent adsorbents. It can be seen from

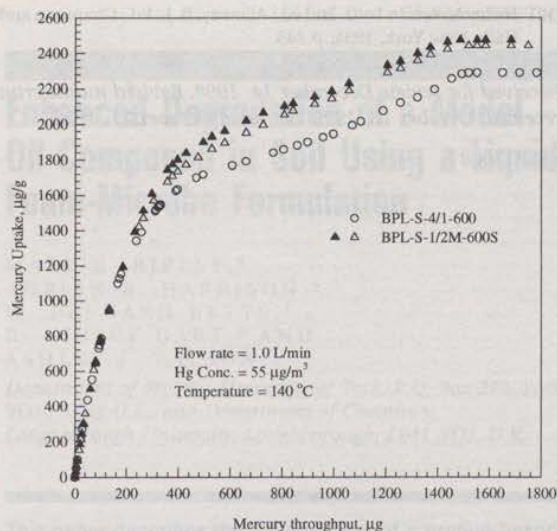


FIGURE 4. Mercury uptake by sulfur-impregnated carbons prepared using two different procedures.

TABLE 2. Properties of Different Particle Size Fractions of BPL-S-4/1-600

particle size [U.S. mesh]	mean particle diameter [mm]	sulfur content [wt %]	specific surface area [m <sup>2</sup> /g]
60 × 80	0.21	10.04–10.18	823.7–845.7
170 × 230	0.08	9.88–10.51	833.7–869.2
minus 400	0.03	10.22–10.56	840.1–852.5

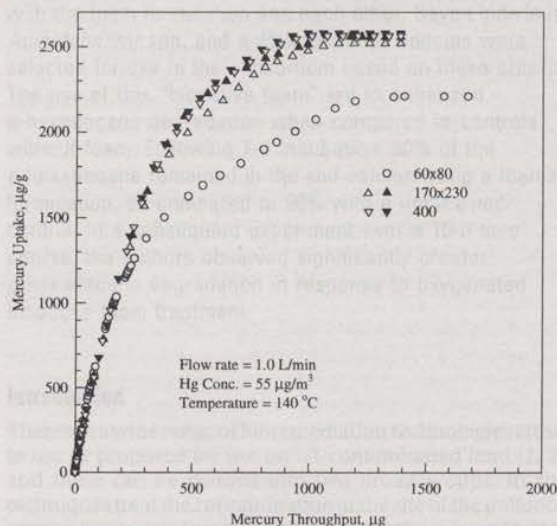


FIGURE 5. Effect of particle size on mercury uptake by BPL-S-4/1-600.

this table that the amount of mercury extracted by acidic solution is below the detection limit of the analytical method used (about 0.1–0.2 µg/L). The sample storage time varied from 2 to 330 days, and the adsorbents included all types of sulfur-impregnated carbons (5, 6) (i.e., HGR, React-A-S, and BPL-S series). The last column in Table 3 shows the ratio of the expected mercury mass on adsorbents after breakthrough tests and the amount of mercury measured by combusting the adsorbents after the TCLP test. These results revealed that the amount of mercury remaining on sulfur-impregnated

TABLE 3. TCLP Results for Different Carbon Samples

sample	storage time [days]	Hg in leachate [µg/L]	expected: measured [µg/g carbon]
BPL-S-4/1-600	30	not detected	2287:2170
BPL-S-4/1-600	330	not detected	2312:2421
BPL-S-2/1-600	240	not detected	2010:1907
BPL-S-1/1-600	200	not detected	1256:1302
BPL-S-4/1-400	260	not detected	1448:1331
BPL-S-4/1-250	180	not detected	550:603
React-A-S	300	not detected	1905:1961
HGR	260	not detected	38:36
HGR	60	not detected	36.9:38
BPL	310	<0.2	0.65:0.42
BPL	2	<0.2	0.68:0.71

adsorbents after prolonged storage and after TCLP test was equal to the amount of mercury adsorbed during the breakthrough test.

The test results for BPL carbons loaded with mercury and stored for 2 and 310 days revealed different behavior. Although there was no mercury detected in the TCLP leachate, the combustion tests showed that the amount of mercury present on this adsorbent after 310 days of storage was much lower than the expected value, while the amount of mercury present on BPL carbon after 2 days of storage was within the experimental error of the expected value.

The results described above are in agreement with the hypothesis that mercury is chemisorbed by sulfur-impregnated carbons as HgS. HgS is a very stable chemical with high sublimation point (583.5 °C) and is not soluble in water and weak acids (10).

Although TCLP results showed that the amount of mercury extracted from carbons were far below the RCRA limit (200 µg/L) (11, 12), the stability of mercury on the adsorbent surface is strongly related to the adsorption mechanism and predominant mercury forms.

Apparently, mercury adsorbed by sulfur-impregnated carbons is more stable than that adsorbed by virgin carbons. It is obvious that converting elemental mercury to HgS would be beneficial in terms of handling the spent adsorbents. Another important conclusion is that although TCLP analysis of spent virgin carbon may pass the regulatory limit, the elemental mercury could re-enter the vapor phase during a long storage time. This will certainly present a threat to the environment, and the spent virgin carbon may have to be treated as hazardous waste regardless of the TCLP results.

### Acknowledgments

Funding for this work was provided by the U.S. Department of Energy (Grant No. DE-FG22-96PC96212). The views expressed are entirely those of the authors and do not necessarily reflect the views of the agency. Mention of trade names or commercial products does not constitute endorsement or recommendation for use.

### Literature Cited

- (1) Johnson, J. *Environ. Sci. Technol.* **1997**, *31*, 218A.
- (2) Chu, P.; Porcella, D. B. *Water, Air, Soil Pollut.* **1995**, *80*, 135.
- (3) Chang, R.; Owens, D. *EPRI J.* July/August **1994**, 46.
- (4) Vidic, R. D.; McLaughlin, J. B. *J. Air Waste Manage. Assoc.* **1996**, *46*, 241.
- (5) Korpel, A. J.; Vidic, R. D. *Environ. Sci. Technol.* **1997**, *31*, 2319.
- (6) Liu, W.; Vidic, R. D.; Brown, T. D. *Environ. Sci. Technol.* **1998**, *32*, 531.
- (7) *Chemistry and Physics of Carbon*; Walker, P. L., Jr., Ed.; Vol. 6, Marcel Dekker: New York, 1970; p 264.
- (8) Sykes, K. W.; White, P. *Trans. Faraday Soc.* **1956**, *52*, 660.

- (9) Pouchert, C. J. ed., *The Aldrich Library of FT-IR Spectra Vapor Phase*, 1st ed.; Aldrich Chemical Co.: Milwaukee, WI, 1989; p 343.
- (10) Lide, D. R., ed., *Handbook of Chemistry and Physics*, 73rd ed.; CRC Press: Boca Raton, FL, 1992; pp 4-74.
- (11) U.S. EPA. *Mercury and Arsenic Wastes - - Removal, Recovery, Treatment, and Disposal*; Noyes Data Corporation: Park Ridge, NJ, 1993; p 14.

- (12) *Heavy Metals in Soils*, 2nd ed.; Alloway, B. J., Ed.; Chapman and Hall: New York, 1995; p 245.

Received for review December 14, 1998. Revised manuscript received October 18, 1999. Accepted October 21, 1999.

ES9813008

Wavelength (nm)	Intensity (a.u.)	Wavelength (nm)	Intensity (a.u.)
200	0.0	200	0.0
210	0.0	210	0.0
220	0.0	220	0.0
230	0.0	230	0.0
240	0.0	240	0.0
250	0.0	250	0.0
260	0.0	260	0.0
270	0.0	270	0.0
280	0.0	280	0.0
290	0.0	290	0.0
300	0.0	300	0.0
310	0.0	310	0.0
320	0.0	320	0.0
330	0.0	330	0.0
340	0.0	340	0.0
350	0.0	350	0.0
360	0.0	360	0.0
370	0.0	370	0.0
380	0.0	380	0.0
390	0.0	390	0.0
400	0.0	400	0.0

The amount of mercury released during the test was determined by measuring the amount of mercury in the effluent water.

The test results for BPL indicate that the amount of mercury released during the test was significantly higher than that reported in the literature for other types of BPL.

The results described above are in agreement with the results reported in the literature for other types of BPL.

The results described above are in agreement with the results reported in the literature for other types of BPL.

The results described above are in agreement with the results reported in the literature for other types of BPL.

The results described above are in agreement with the results reported in the literature for other types of BPL.

The results described above are in agreement with the results reported in the literature for other types of BPL.



Figure 1. Mercury release from integrated carbon prepared using two different procedures.

TABLE 1. Properties of Different Particle Size Fractions of BPL-2-11500

Particle size (μm)	Specific surface area (m <sup>2</sup> /g)	Volume fraction (%)	Mass fraction (%)
0.5 - 1.0	1000 - 1500	10	5
1.0 - 2.0	500 - 1000	20	10
2.0 - 5.0	200 - 500	30	15
5.0 - 10.0	100 - 200	20	10
10.0 - 20.0	50 - 100	10	5
20.0 - 50.0	20 - 50	5	2.5
50.0 - 100.0	10 - 20	2	1
100.0 - 200.0	5 - 10	1	0.5
200.0 - 500.0	2 - 5	0.5	0.25
500.0 - 1000.0	1 - 2	0.2	0.1
1000.0 - 2000.0	0.5 - 1	0.1	0.05
2000.0 - 5000.0	0.2 - 0.5	0.05	0.025
5000.0 - 10000.0	0.1 - 0.2	0.02	0.01
10000.0 - 20000.0	0.05 - 0.1	0.01	0.005
20000.0 - 50000.0	0.02 - 0.05	0.005	0.0025
50000.0 - 100000.0	0.01 - 0.02	0.002	0.001
100000.0 - 200000.0	0.005 - 0.01	0.001	0.0005
200000.0 - 500000.0	0.002 - 0.005	0.0005	0.00025
500000.0 - 1000000.0	0.001 - 0.002	0.0002	0.0001
1000000.0 - 2000000.0	0.0005 - 0.001	0.0001	0.00005
2000000.0 - 5000000.0	0.0002 - 0.0005	0.00005	0.000025
5000000.0 - 10000000.0	0.0001 - 0.0002	0.00002	0.00001
10000000.0 - 20000000.0	0.00005 - 0.0001	0.00001	0.000005
20000000.0 - 50000000.0	0.00002 - 0.00005	0.000005	0.0000025
50000000.0 - 100000000.0	0.00001 - 0.00002	0.000002	0.000001
100000000.0 - 200000000.0	0.000005 - 0.00001	0.000001	0.0000005
200000000.0 - 500000000.0	0.000002 - 0.000005	0.0000005	0.00000025
500000000.0 - 1000000000.0	0.000001 - 0.000002	0.0000002	0.0000001
1000000000.0 - 2000000000.0	0.0000005 - 0.000001	0.0000001	0.00000005
2000000000.0 - 5000000000.0	0.0000002 - 0.0000005	0.00000005	0.000000025
5000000000.0 - 10000000000.0	0.0000001 - 0.0000002	0.00000002	0.00000001
10000000000.0 - 20000000000.0	0.00000005 - 0.0000001	0.00000001	0.000000005
20000000000.0 - 50000000000.0	0.00000002 - 0.00000005	0.000000005	0.0000000025
50000000000.0 - 100000000000.0	0.00000001 - 0.00000002	0.000000002	0.000000001
100000000000.0 - 200000000000.0	0.000000005 - 0.00000001	0.000000001	0.0000000005
200000000000.0 - 500000000000.0	0.000000002 - 0.000000005	0.0000000005	0.00000000025
500000000000.0 - 1000000000000.0	0.000000001 - 0.000000002	0.0000000002	0.0000000001
1000000000000.0 - 2000000000000.0	0.0000000005 - 0.000000001	0.0000000001	0.00000000005
2000000000000.0 - 5000000000000.0	0.0000000002 - 0.0000000005	0.00000000005	0.000000000025
5000000000000.0 - 10000000000000.0	0.0000000001 - 0.0000000002	0.00000000002	0.00000000001
10000000000000.0 - 20000000000000.0	0.00000000005 - 0.0000000001	0.00000000001	0.000000000005
20000000000000.0 - 50000000000000.0	0.00000000002 - 0.00000000005	0.000000000005	0.0000000000025
50000000000000.0 - 100000000000000.0	0.00000000001 - 0.00000000002	0.000000000002	0.000000000001
100000000000000.0 - 200000000000000.0	0.000000000005 - 0.00000000001	0.000000000001	0.0000000000005
200000000000000.0 - 500000000000000.0	0.000000000002 - 0.000000000005	0.0000000000005	0.00000000000025
500000000000000.0 - 1000000000000000.0	0.000000000001 - 0.000000000002	0.0000000000002	0.0000000000001
1000000000000000.0 - 2000000000000000.0	0.0000000000005 - 0.000000000001	0.0000000000001	0.00000000000005
2000000000000000.0 - 5000000000000000.0	0.0000000000002 - 0.0000000000005	0.00000000000005	0.000000000000025
5000000000000000.0 - 10000000000000000.0	0.0000000000001 - 0.0000000000002	0.00000000000002	0.00000000000001
10000000000000000.0 - 20000000000000000.0	0.00000000000005 - 0.0000000000001	0.00000000000001	0.000000000000005
20000000000000000.0 - 50000000000000000.0	0.00000000000002 - 0.00000000000005	0.000000000000005	0.0000000000000025
50000000000000000.0 - 100000000000000000.0	0.00000000000001 - 0.00000000000002	0.000000000000002	0.000000000000001
100000000000000000.0 - 200000000000000000.0	0.000000000000005 - 0.00000000000001	0.000000000000001	0.0000000000000005
200000000000000000.0 - 500000000000000000.0	0.000000000000002 - 0.000000000000005	0.0000000000000005	0.00000000000000025
500000000000000000.0 - 1000000000000000000.0	0.000000000000001 - 0.000000000000002	0.0000000000000002	0.0000000000000001
1000000000000000000.0 - 2000000000000000000.0	0.0000000000000005 - 0.000000000000001	0.0000000000000001	0.00000000000000005
2000000000000000000.0 - 5000000000000000000.0	0.0000000000000002 - 0.0000000000000005	0.00000000000000005	0.000000000000000025
5000000000000000000.0 - 10000000000000000000.0	0.0000000000000001 - 0.0000000000000002	0.00000000000000002	0.00000000000000001
10000000000000000000.0 - 20000000000000000000.0	0.00000000000000005 - 0.0000000000000001	0.00000000000000001	0.000000000000000005
20000000000000000000.0 - 50000000000000000000.0	0.00000000000000002 - 0.00000000000000005	0.000000000000000005	0.0000000000000000025
50000000000000000000.0 - 100000000000000000000.0	0.00000000000000001 - 0.00000000000000002	0.000000000000000002	0.000000000000000001
100000000000000000000.0 - 200000000000000000000.0	0.000000000000000005 - 0.00000000000000001	0.000000000000000001	0.0000000000000000005
200000000000000000000.0 - 500000000000000000000.0	0.000000000000000002 - 0.000000000000000005	0.0000000000000000005	0.00000000000000000025
500000000000000000000.0 - 1000000000000000000000.0	0.000000000000000001 - 0.000000000000000002	0.0000000000000000002	0.0000000000000000001
1000000000000000000000.0 - 2000000000000000000000.0	0.0000000000000000005 - 0.000000000000000001	0.0000000000000000001	0.00000000000000000005
2000000000000000000000.0 - 5000000000000000000000.0	0.0000000000000000002 - 0.0000000000000000005	0.00000000000000000005	0.000000000000000000025
5000000000000000000000.0 - 10000000000000000000000.0	0.0000000000000000001 - 0.0000000000000000002	0.00000000000000000002	0.00000000000000000001
10000000000000000000000.0 - 20000000000000000000000.0	0.00000000000000000005 - 0.0000000000000000001	0.00000000000000000001	0.000000000000000000005
20000000000000000000000.0 - 50000000000000000000000.0	0.00000000000000000002 - 0.00000000000000000005	0.000000000000000000005	0.0000000000000000000025
50000000000000000000000.0 - 100000000000000000000000.0	0.00000000000000000001 - 0.00000000000000000002	0.000000000000000000002	0.000000000000000000001
100000000000000000000000.0 - 200000000000000000000000.0	0.000000000000000000005 - 0.00000000000000000001	0.000000000000000000001	0.0000000000000000000005
200000000000000000000000.0 - 500000000000000000000000.0	0.000000000000000000002 - 0.000000000000000000005	0.0000000000000000000005	0.00000000000000000000025
500000000000000000000000.0 - 1000000000000000000000000.0	0.000000000000000000001 - 0.000000000000000000002	0.0000000000000000000002	0.0000000000000000000001
1000000000000000000000000.0 - 2000000000000000000000000.0	0.0000000000000000000005 - 0.000000000000000000001	0.0000000000000000000001	0.00000000000000000000005
2000000000000000000000000.0 - 5000000000000000000000000.0	0.0000000000000000000002 - 0.0000000000000000000005	0.00000000000000000000005	0.000000000000000000000025
5000000000000000000000000.0 - 10000000000000000000000000.0	0.0000000000000000000001 - 0.0000000000000000000002	0.00000000000000000000002	0.00000000000000000000001
10000000000000000000000000.0 - 20000000000000000000000000.0	0.00000000000000000000005 - 0.0000000000000000000001	0.00000000000000000000001	0.000000000000000000000005
20000000000000000000000000.0 - 50000000000000000000000000.0	0.00000000000000000000002 - 0.00000000000000000000005	0.000000000000000000000005	0.0000000000000000000000025
50000000000000000000000000.0 - 100000000000000000000000000.0	0.00000000000000000000001 - 0.00000000000000000000002	0.000000000000000000000002	0.000000000000000000000001
100000000000000000000000000.0 - 200000000000000000000000000.0	0.000000000000000000000005 - 0.00000000000000000000001	0.000000000000000000000001	0.0000000000000000000000005
200000000000000000000000000.0 - 500000000000000000000000000.0	0.000000000000000000000002 - 0.000000000000000000000005	0.0000000000000000000000005	0.00000000000000000000000025
500000000000000000000000000.0 - 1000000000000000000000000000.0	0.000000000000000000000001 - 0.000000000000000000000002	0.0000000000000000000000002	0.0000000000000000000000001
1000000000000000000000000000.0 - 2000000000000000000000000000.0	0.0000000000000000000000005 - 0.000000000000000000000001	0.0000000000000000000000001	0.00000000000000000000000005
2000000000000000000000000000.0 - 5000000000000000000000000000.0	0.0000000000000000000000002 - 0.0000000000000000000000005	0.00000000000000000000000005	0.000000000000000000000000025
5000000000000000000000000000.0 - 10000000000000000000000000000.0	0.0000000000000000000000001 - 0.0000000000000000000000002	0.00000000000000000000000002	0.00000000000000000000000001
10000000000000000000000000000.0 - 20000000000000000000000000000.0	0.00000000000000000000000005 - 0.0000000000000000000000001	0.00000000000000000000000001	0.000000000000000000000000005
20000000000000000000000000000.0 - 50000000000000000000000000000.0	0.00000000000000000000000002 - 0.00000000000000000000000005	0.000000000000000000000000005	0.0000000000000000000000000025